

# Soft QCD Effects in VBS/VBF Topologies

Carsten Bittrich<sup>1</sup>, Patrick Kirchga  er<sup>2</sup>, Andreas Papaefstathiou<sup>3</sup>, Simon Pl  tzer<sup>4,5,6</sup> and Stefanie Todt<sup>1</sup>

<sup>1</sup> Institut f  r Kern- und Teilchenphysik, TU Dresden, Dresden, Germany

<sup>2</sup> Theoretical Particle Physics, Department of Astronomy and Theoretical Physics, Lund University, Lund, Sweden

<sup>3</sup> Department of Physics, Kennesaw State University, Kennesaw, GA 30144, USA

<sup>4</sup> Institute of Physics, NAWI Graz, University of Graz, Universit  tsplatz 5, A-8010 Graz, Austria

<sup>5</sup> Particle Physics, Faculty of Physics, University of Vienna, Boltzmanngasse 5, A-1090 Wien, Austria

<sup>6</sup> Erwin Schr  dinger Institute for Mathematics and Physics, University of Vienna, Boltzmanngasse 9, A-1090 Wien, Austria

October 6, 2021

**Abstract.** We consider the impact of multi-parton interactions, colour reconnection and hadronization on the modeling of vector boson fusion and vector boson scattering (VBS) final states at the Large Hadron Collider (LHC). We investigate how the variation of the model parameters, compatible with a reasonable spread of predictions around typical tuning observables, extrapolates into the VBS phase space. We study the implications of this variation on the total uncertainty budget attached to realistic simulation of the final states in current event generator predictions. We find that the variations have a non-trivial phase space dependence and become comparable in size to the perturbative uncertainties once next-to-leading order predictions are combined with parton shower evolution.

## 1 Introduction

An accurate description of the complex final states at the LHC is vital to distinguish New Physics from those already encompassed by the Standard Model. After the discovery of the Higgs boson, one focus of the ongoing and future runs of the LHC is to precisely unravel the physics of electroweak Higgs boson production, and the interactions of weak gauge bosons themselves at high energies. This is key to understanding the mechanism of electroweak symmetry breaking and the Higgs boson properties, beyond those established so far.

While the processes of interest, vector boson fusion (VBF) into a Higgs boson, or vector boson scattering (VBS) more generally, are genuine electroweak processes, at a hadron collider, they will be triggered at significant rates only if the strongly-interacting quarks are involved, and as such QCD dynamics is unavoidable within this class of processes. In particular, the expected final state consists of a pair of highly-energetic jets originating from the quarks that initiated the electroweak process, and little hadronic activity is expected elsewhere due to the lack of exchange of colour charge in between the so-called tagging jets [1, 2]. These VBF, or VBS signatures (we will not distinguish between VBF and VBS in the following), however, will necessarily interfere with QCD-induced processes, and even as fixed-order electroweak processes, they will not necessarily be dominated by contributions from diagrams with a VBS topology, *i.e.* a colour-less exchange in the  $t$ -channel of the hard scattering. They will also interfere with processes that have initial state ( $s$ -channel) or

$u$ -channel colour connections, as well. These effects can be shown to be suppressed kinematically in the phase space region exhibiting the VBS signatures by including a veto on additional hadronic activity in between the tagging jets [3].

Accepting the VBS approximation, *i.e.* neglecting the interferences and other topologies within the acceptance of interest, as a reliable way of predicting the final states, one indeed finds stunningly small QCD uncertainties at fixed order [4, 5], even including a third jet *e.g.* in VBF Higgs production [6]. A similar statement is true when including the effects of jet evolution as commonly implemented in multi-purpose event generators and matched to next-to-leading order (NLO) QCD predictions [7]. The jet radius dependence of the VBS cross sections has also been studied carefully in a quest for more perturbative stability. Numerically significant effects of QCD colour singlet exchanges not covered by NNLO calculations in the  $t$ -channel approximation, nor included in readily available parton shower algorithms<sup>1</sup> have been pointed out in the literature [3]. However, for the currently-available state of the art, one would consider these processes to be theoretically accurate and precisely modeled at NLO QCD, at least within the typical region of VBS acceptance. The merging of different jet multiplicities has recently been addressed in VBF Higgs production [9, 10], and detailed studies of parton shower effects are available in these cases [11, 12], suggesting that the perturbative

<sup>1</sup> Exceptions of this kind are newly developed evolution algorithms at the amplitude level, see *e.g.* [8].

component is mostly well under control, though [10] has in fact pointed out that the role of the VBF approximation in shower initial conditions for multi-jet merging might be more delicate than naively expected.

In this work, we point out that gaining control of the perturbative part of the prediction and the realistic simulation of the final states of interest is a necessary ingredient to an uncertainty budget of theoretical modeling, however by far not a sufficient one. We therefore address the effect of dynamics in a proton-proton collision which has not been accounted for in studies performed so far and are typically outside a ready-to-use concept of estimating the impact of neglected contributions and missing higher order corrections: those are the physics of multi-parton interactions, hadronization, and colour reconnection which we believe represent specifically important effects, particularly in light of the distinct character of the VBS processes, as well as the open question of the role of non-trivial QCD effects originating from colour evolution [13, 14].

While one would in fact expect that the overall impact of the physics addressed in this work would not lead to tremendous effects, care needs to be taken that variations within these contributions might become comparable to the level of uncertainty reached by the perturbative description, including a non-trivial phase space dependence. This is something we need to accept will happen even in light of minimum bias and underlying event data of small uncertainties predicted very well by these models. It is the purpose of the present work to explicitly check for the size of variations of the non-perturbative models and to clarify whether their impact relative to the perturbative part sets a reliable scale on the uncertainty one should expect.

This manuscript is structured as follows: In Sec. 2 we will review the overall uncertainty budget of an event generator simulation, mostly following the lines of [15], however with a focus on multi-parton interaction (MPI) modeling, and the role of phenomenological models of colour reconnection and hadronization. In Sec. 3 we will then outline the simulation used in this study, which has been mainly based on the VBFNLO library [16–18] and the Herwig 7 event generator [19, 20], though we do not expect that any of our initial reasoning and findings are indeed specific to the models implemented within Herwig and would equally well apply to any other event generator. In Sec. 4 we study the impact of MPI, and variations of the MPI model, onto VBS final states for the first time, before we present conclusions and an outlook into future work.

## 2 Overview on Event Generator Uncertainties

While there are very well established methods of estimating the uncertainty of fixed-order and analytically resummed perturbative calculations due to missing higher orders, the same concept does not exist in one-to-one correspondence for even the perturbative parts of event generators. Progress has been made, though, in varying the scales involved in the parton shower evolution as well as the matching algorithms [15, 21] and can now be deemed

a reliable measure of parton shower uncertainty, included along with variations in the hard process. A strong analytic statement is not possible in these cases, owing to the fact that analytic insight into parton shower-evolved observables is typically lacking.

What parton shower variations typically assess is the reliability of predictions in phase space regions populated by parton shower emissions, and how a poor description of such regions is improved by matching and merging. To this extent, we can speak of reliable perturbative input. However, as the perturbative parton shower evolution does bridge the gap to the small scales at which phenomenological models take over, these variations cannot make up the entire uncertainty budget of an event generator and need to be confronted with the reliability of models of soft physics – describing multi-parton interactions, colour reconnection and hadronization – and their interplay needs to be carefully evaluated. On the perturbative side, to be precise, we build on the findings of [22], and use LO- and NLO-matched simulations, varying the shower hard scale but not the profile function by which the hard end of shower emissions’ phase space is approached, and using the ‘resummation profile’ advocated in [15] to preserve the properties we demand by a combination of hard process and parton shower. We do not consider any parametric uncertainties such as variations in the strong coupling or parton distribution functions.

In the remainder of this section we will focus on MPI and colour reconnection models, which are vital to describe the complexity observed in hadronic collisions. The parameters of these models, to be discussed in detail below, are typically tuned to observables which are designed to probe the additional activity introduced by multi-parton interactions, at scales smaller than the typical momentum transfer of the hard scattering of interest. By virtue of their abundant occurrence, these observables have very small experimental uncertainty, and models deliver enough parameters and dynamics to deliver a decent fit of those data. The goodness-of-fit can be quantified using standard methods and is now conveniently available in form of so-called ‘Eigentunes’ [23]. However, those measures of uncertainty cannot reflect how precise we believe these models are, nor how accurate they are outside the range of observables typically considered for the soft physics tunes.

The MPI model is crucial for “dressing” the signal process with additional hadronic activity. The underlying event activity is modeled as perturbative QCD  $2 \rightarrow 2$  processes and additional soft interactions simulated as multiperipheral particle production [24–28]. Here we give a quick overview of the main concepts of interest for the discussion in later sections. At the beginning of a run with Herwig, the MPI model determines a matrix containing the probabilities for the different number of  $h$  hard and  $n$  soft interactions

$$P_{h,n}(s) = \frac{\sigma_{h,n}(s)}{\sigma_{\text{inel}}(s)}, \quad (1)$$

where  $\sigma_{\text{inel}}(s)$  is the inelastic non-diffractive cross section and  $\sigma_{h,n}(s)$  is the cross section for  $h$  hard and  $n$  soft events

$$\sigma_{h,n}(s) = \int d^2\mathbf{b} \frac{\langle n(b,s) \rangle_{\text{hard}}^h}{h!} \frac{\langle n(b,s) \rangle_{\text{soft}}^n}{n!} \times e^{-\langle n(b,s) \rangle_{\text{hard}} + \langle n(b,s) \rangle_{\text{soft}}} . \quad (2)$$

The number of soft and hard interactions follow a Poissonian distribution with mean values

$$\langle n(b,s) \rangle_{\text{hard}} = A(b, \mu_{\text{hard}}) \sigma_{\text{hard}}^{\text{inc}}(p_{\perp}^{\text{min}}, s) \quad (3)$$

and

$$\langle n(b,s) \rangle_{\text{soft}} = A(b, \mu_{\text{soft}}) \sigma_{\text{soft}}^{\text{inc}}(s) . \quad (4)$$

$A(b, \mu)$  is the overlap function given by

$$A(b, \mu) = \frac{\mu^2}{96\pi} (\mu b)^3 K_3(\mu b) , \quad (5)$$

where  $K_3$  is the modified Bessel function of the second kind. The overlap function has a different form for soft and hard interactions since we assume that the interactions depend on different matter distributions inside the proton.  $\sigma_{\text{hard}}^{\text{inc}}(p_{\perp}^{\text{min}}, s)$  is the inclusive cross section for QCD  $2 \rightarrow 2$  processes above  $p_{\perp}^{\text{min}}$ , calculable in perturbative QCD. The soft inclusive cross section  $\sigma_{\text{soft}}^{\text{inc}}(s)$  and the soft inverse proton radius  $\mu_{\text{soft}}$  are chosen such that the total cross section  $\sigma_{\text{tot}}(s)$  is correctly described.<sup>2</sup>

The Herwig MPI model has two main genuine free parameters. These are the hard inverse proton radius  $\mu_{\text{hard}}$  and the minimum transverse momentum  $p_{\perp}^{\text{min}}$ , which factorizes hard and soft interactions in terms of  $p_{\perp}$ .

For the accurate description of minimum bias data and flavour observables additional non-perturbative effects like colour reconnection must be taken into account [30, 31]. Colour reconnection is used in this regard to restore the notion of a pre-confined state [30] in the presence of extreme event topologies where many overlapping clusters from multiple parton interactions are encountered. After the evolution of the parton shower has terminated, colour-preconfinement states that colour connected partons are close in momentum space, which leads to a distribution of invariant cluster masses peaking at small values of  $M$ . The *plain* colour reconnection algorithm in Herwig tries to find configurations of clusters that reduce the sum of invariant cluster masses

$$\lambda = \sum_{i=1}^{N_{cl}} M_i^2 . \quad (6)$$

The algorithm picks a cluster randomly from the list of clusters and compares it to all other clusters in the event. The invariant mass of the alternative cluster configuration is calculated and, if this leads to a reduction in the sum of cluster masses, this configuration is accepted with a fixed probability  $p_{\text{Reco}}$ .

<sup>2</sup> The total cross section is determined with the Donnachie-Landshoff parametrization [29].

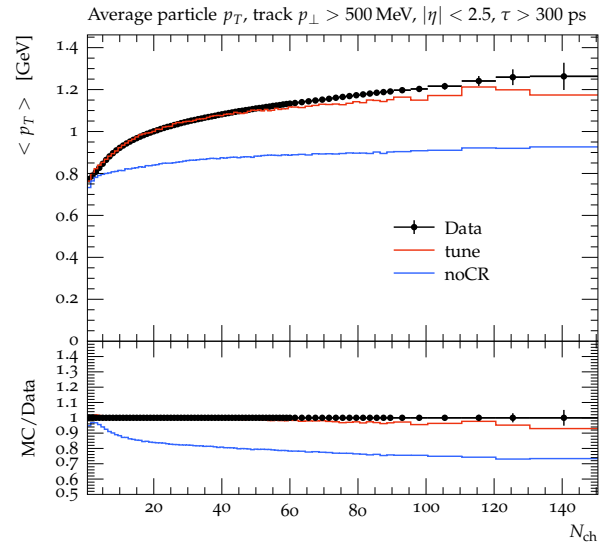


Fig. 1:  $\langle p_{\perp} \rangle$  vs.  $N_{\text{ch}}$ . Measured by [34]. The distribution is not described without a colour reconnection mechanism.

Models represent our lack of exact knowledge about the physics in question in the non-perturbative regime. There is no clear true/false distinction between models possible. Rather, the evaluation of a model's quality follows along the lines of better/worse. A puzzling question in the context of these models, which are often inspired by theoretical principles concerns the correct assessment of uncertainties. The assessment of uncertainties for non-perturbative models is in general an ill-defined problem.

“On-off” studies that involve the relevant parts of the model are frequently used, for example to assess the impact of colour reconnection or any other model that modifies the final state of the simulation [32]. While this is a sensible approach to study the effects of the model, minimum bias data clearly shows that colour reconnection is a necessary ingredient in order to describe the data (see fig. 1 and [33]). Therefore, turning off colour reconnection means ignoring important physics effects, which implies that the on-off technique is not suited to discuss the propagation of model uncertainties to VBF observables.

### 3 Outline of the Simulation

As an example process we consider Vector Boson Fusion  $Z$  production, *i.e.*  $pp \rightarrow \mu^+ \mu^- + 2 \text{ jets}$ , since this is one of the most relevant processes within current analyses and allows us to closely follow the experimental acceptances. In this work we consider the ‘signal’ process mediated by electroweak interactions at tree level and supplemented by NLO QCD corrections in the VBF approximation as implemented in the VBFNLO library. VBFNLO has been interfaced to Herwig 7 and we perform the matching to NLO QCD using the Matchbox framework [35] through the MC@NLO-type matching paradigm to the angular ordered shower. In what follows, we will refer to these simulations as ‘NLO’. As a cross check on the simulation of the

perturbative structures, we also consider a simulation using tree-level merging based on MadGraph-generated amplitudes [36] and merged with the dipole shower of Herwig following the method outlined in [37, 38]. This simulation has the same – leading order – accuracy for the description of the third jet, and we can further test if the VBF approximation is valid in this study. It is vital that we can reduce the uncertainties of the modeling of the third jet to actually observe the impact of soft QCD variations on jet veto observables. These would otherwise be mismodeled as reflected in large parton shower variations in the case of the third jet not predicted by an exact matrix element.

Since we are considering the VBF approximation for most of this study, we do require to set up the analysis using the VBF phase space region of two energetic tagging jets at large invariant mass and rapidity separation. Since this selection is not enforced as strictly as one would feel comfortable with theoretically, we chose a tight and a loose VBF cut setup, to probe the transition region towards which the VBF approximation would not be considered to be very reliable. To be specific, both sets of cuts require jets to be defined with the anti- $k_{\perp}$  algorithm [39], with

$$p_{\perp,j} > 25 \text{ GeV}, \quad |y_j| < 4.5, \quad (7)$$

and a minimum of two jets. For these two jets, the ‘loose’ setup requires

$$m_{12} > 250 \text{ GeV}, \quad \Delta y_{12} > 0.0, \quad (8)$$

while the ‘tight’ setup requires

$$m_{12} > 1000 \text{ GeV}, \quad \Delta y_{12} > 2.0. \quad (9)$$

In order to evaluate the perturbative uncertainties, we vary the renormalization and factorization scales by a factor  $\sqrt{2}$  around their central value, which are given by the  $H_{\perp}$  of the hard scattering

$$\mu_{R,F} = M_{\perp}(Z) + \sum_{i \in \text{jets}} p_{\perp,i}. \quad (10)$$

These scales, but not their variations, set the hard scale above which shower emissions are vetoed for the shower not to produce radiation above the typical scales of the jets involved in the hard process. The transition towards the hard phase space is implemented using the ‘resummation profile’ as discussed in [15], and the shower hard scale is then varied individually with  $\pm\sqrt{2}\mu_{R,F}$  to obtain an estimate on how reliable the shower predictions are in certain regions.

As far as the non-perturbative variations are concerned, we follow the approach to tune the MPI and colour reconnection model to 13 TeV underlying event data from Ref. [40] and then find variations in the parameter space which correspond to a  $\sim 10\%$  band around the tuned values. We then proceed to study how these parameter variations propagate to perturbative VBF observables. The tuned parameter values and the corresponding parameter variations are shown in Tab. 1. By varying the param-

	tune	up	down
$p_{\perp}^{\min}$	3.19	3.4	2.9
$\mu_{\text{hard}}$	0.92	1.2	0.75
$p_{\text{Reco}}$	0.63	0.8	0.4

Table 1: Tuned parameter values and parameter variations.

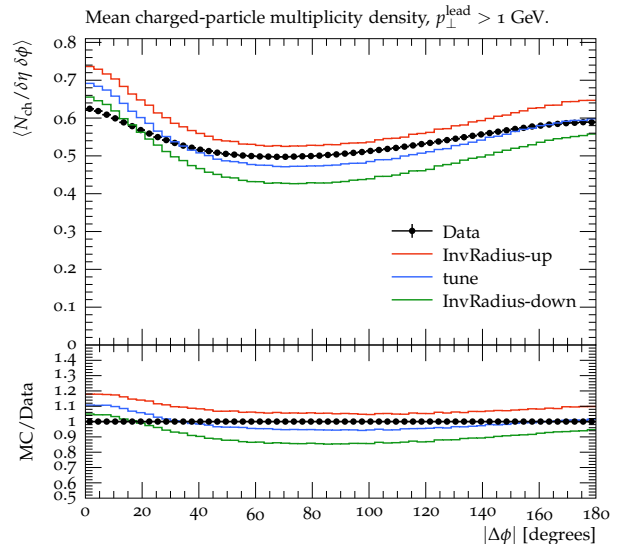


Fig. 2: Plot of the mean charged particle multiplicity with respect to the difference in the azimuth angle  $\Delta\Phi$  [40] for the tuned parameter values and the  $\mu_{\text{hard}}$  variations. The variations cover roughly a  $\sim 10\%$  band around the description with the tuned parameter values.

eters we still have all the physical mechanisms incorporated in the simulation. We performed LO and NLO simulations for the full set of parameter variations. The results of these simulations, including additional observables to those presented in this article, as well as the Rivet analysis [41] code used can be found at the accompanying web page [42]. We find that the up and down variations of the inverse proton radius  $\mu_{\text{hard}}$  constitutes the outermost variations of the third-leading jet VBF observables. Therefore, this parameter is especially suited for our purposes since it is directly correlated with the amount of underlying event activity induced from MPI processes (see fig. 2).

## 4 Impact of Multi-parton Interactions

We have performed an investigation of the net impact of the different model components on the final result of the simulation. In particular, we found that the contribution of multi-parton interactions is significant and rises with increasing jet radius, as one would expect. This is especially true for distributions of the third jet, and possibly higher jet multiplicities, which we have not been investigating in great detail. We observe this both at leading, as well as next-to-leading order matched simulation which implies that we do not mix model contributions with a

lack of higher order corrections. In the following subsections we show the uncertainties in VBF observables due to the outermost variations in the MPI model, which corresponds to the variation of the inverse proton radius  $\mu_{\text{hard}}$  as explained in Sec. 3.

#### 4.1 LO versus NLO

Figure 3 shows a comparison of the LO and NLO third-jet rapidity distributions for various setups: loose and tight selection cuts as described by eqs. 7–9, with jet radius either  $R = 0.4$  or  $R = 0.7$ . The bands shown constitute the outermost variations of the MPI model. The size of this variation is evidently driven by the jet radius, but the size of the NLO correction is essentially independent of the setup. Therefore, in what follows, we only examine distributions at NLO.

#### 4.2 Loose versus tight selection for NLO

In fig. 4 we present a comparison of the NLO VBS third-jet transverse momentum (left) and rapidity (right), between the loose and tight selection cuts for jet radii of  $R = 0.4$  and  $R = 0.7$ , shown in the top and bottom plots, respectively. As before, the bands represent the outermost variations of the MPI model. It can be seen that a tight selection cut setup does not reduce the effects of the MPI. On the contrary, tighter cuts lead to an increase of the uncertainty due to the MPI variations. This is due to the fact that when applying tight cuts, the third jet is forced to become more forward than in the case of loose cuts, effectively making it more sensitive to the soft activity in the event.

#### 4.3 MPI versus Shower variations

We show in fig. 5, a selection of comparisons of the MPI variations and shower variations for NLO VBS observables for the loose (top plots) and tight (bottom plots) selection cuts, for a jet radius of  $R = 0.4$  (left plots) and  $R = 0.7$  (right plots). To reduce the number of plots shown, the transverse momentum and Zeppenfeld variable of the third-leading jet are shown for specific setups. One can observe that the MPI variation becomes more important than the shower variation, particularly for larger jet radii and for tighter selection cuts.

## 5 Conclusion and Outlook

In this study we have presented a first assessment of uncertainties introduced by non-perturbative models in VBF/VBS processes. While there is no a priori recipe on how to quantify such an uncertainty from first principles, we have been taking a pragmatic approach of checking how common sense variations of  $\sim 10\%$  around data typically used

in tunes of the MPI and colour reconnection models extrapolate into a different phase space and class of observables used in VBF/VBS analysis. We find clear evidence that these variations become comparable to, and even outrange, those from the perturbative components in an NLO+PS matched setup. This, in particular, applies to observables of the third-jet activity which is used for central jet vetoes and other analyses targeting the colour structure of the VBF/VBS process. We also find that the variation of the colour reconnection model, which is of crucial importance to the description of MPI activity, does not introduce the most significant variations, and that core parameters of the MPI model are a more relevant source of uncertainty in this context. Our work demonstrates that simply evaluating the contribution of a specific non-perturbative component to the net result of an event generator simulation is not an accurate analysis of uncertainty and a highly phase-space dependent phenomenon. A more detailed analysis would also need to account for the effect of tuning and investigate if there is a tension in between tuning to classes of observables that do or do not involve the VBF phase space. Pending availability of relevant data, we leave this exercise to future work; however one could consider to also do this on the level of some generated data by re-tuning the model parameters at a variation of a single parameter and for different classes of observables.

## Acknowledgments

This work has been initiated within a Short-term Scientific Mission funded by the COST action CA16108 “VBSCAN” at the University of Vienna. CB, PK and ST would like to thank the University of Vienna for their hospitality during this period. PK and SP want to thank the Erwin Schrödinger Institute Vienna for support while this work has been finalized. SP wants to thank the University of Dresden for hospitality where further parts of this study have been discussed. CB and ST have been funded by the German BMBF project 05H2018 “ErUM-FSP T02”. This work has also received funding from the European Union’s Horizon 2020 research and innovation programme as part of the Marie Skłodowska-Curie Innovative Training Network MCnetITN3 (grant agreement no. 722104), and in part by the COST actions CA16201 “PARTICLEFACE”. This work was funded in part by the Knut and Alice Wallenberg foundation, contract number 2017.0036. We are grateful to Stefan Gieseke, Frank Siegert and Dieter Zeppenfeld for useful discussions.

## References

1. D. L. Rainwater and D. Zeppenfeld, *Observing  $H \rightarrow W^*W^* \rightarrow e^\pm \mu^\mp \not{p}_T$  in weak boson fusion with dual forward jet tagging at the CERN LHC*, *Phys. Rev. D* **60** (1999) 113004, [[hep-ph/9906218](#)]. [Erratum: *Phys.Rev.D* **61**, 099901 (2000)].

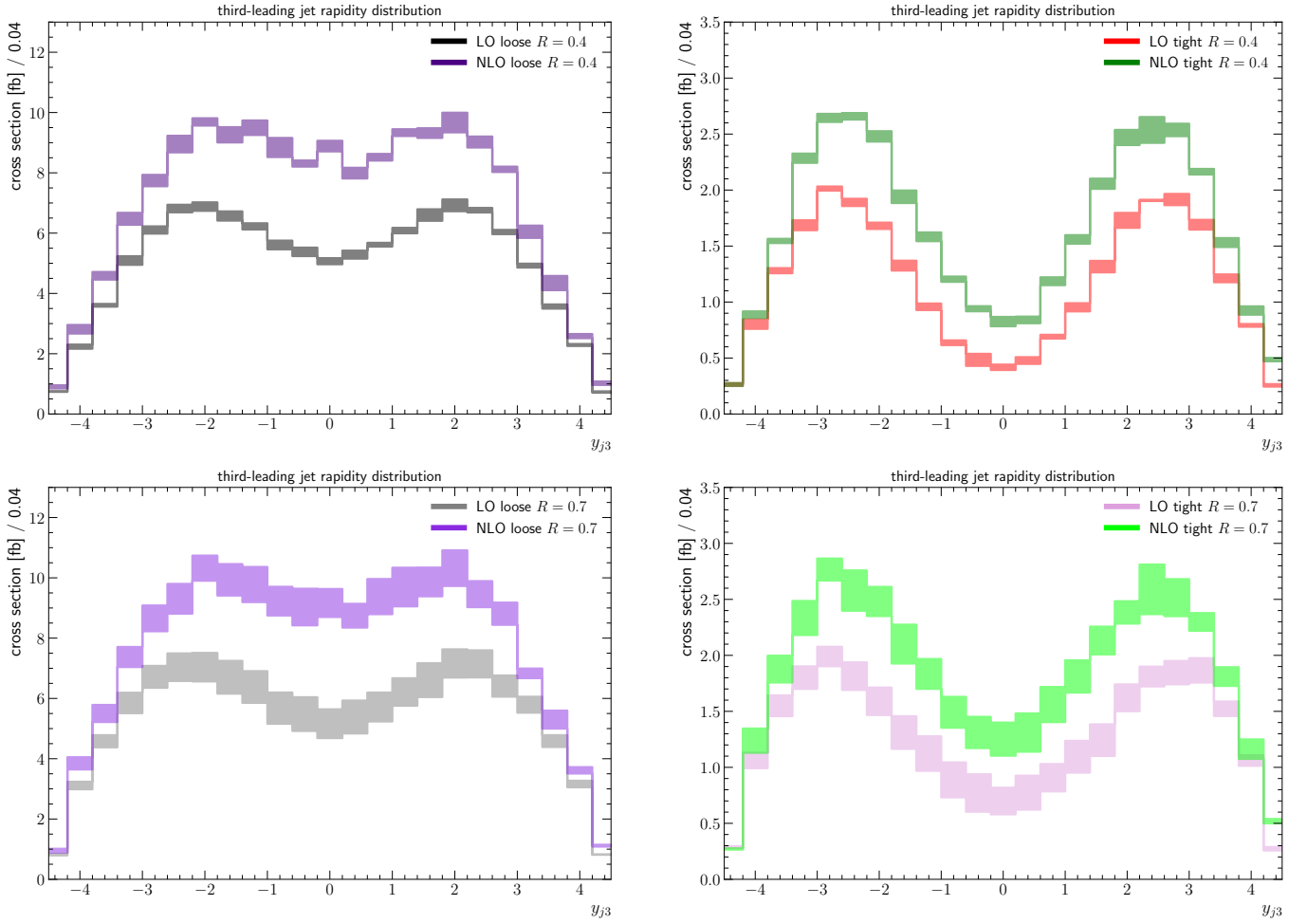


Fig. 3: LO versus NLO VBS third-jet rapidity distributions for the loose (left plots) and tight (right plots) selection cuts for a jet radius of  $R = 0.4$  (top plots) and  $R = 0.7$  (bottom plots). The bands constitute the outermost variations of the MPI model.

2. M. Rauch, *Vector-Boson Fusion and Vector-Boson Scattering*, [arXiv:1610.08420](#).
3. F. Campanario, T. M. Figy, S. Plätzer, M. Rauch, P. Schichtel, and M. Sjö Dahl, *Stress testing the vector-boson-fusion approximation in multijet final states*, *Phys. Rev. D* **98** (2018), no. 3 033003, [[arXiv:1802.09955](#)].
4. C. Oleari and D. Zeppenfeld, *QCD corrections to electroweak  $\nu(l) j j$  and  $l+l-j j$  production*, *Phys. Rev. D* **69** (2004) 093004, [[hep-ph/0310156](#)].
5. B. Jäger, C. Oleari, and D. Zeppenfeld, *Next-to-leading order QCD corrections to  $W+W-$  production via vector-boson fusion*, *JHEP* **07** (2006) 015, [[hep-ph/0603177](#)].
6. T. Figy, V. Hankele, and D. Zeppenfeld, *Next-to-leading order QCD corrections to Higgs plus three jet production in vector-boson fusion*, *JHEP* **02** (2008) 076, [[arXiv:0710.5621](#)].
7. A. Ballestrero et al., *Precise predictions for same-sign  $W$ -boson scattering at the LHC*, *Eur. Phys. J. C* **78** (2018), no. 8 671, [[arXiv:1803.07943](#)].
8. M. De Angelis, J. R. Forshaw, and S. Plätzer, *Resummation and Simulation of Soft Gluon Effects beyond Leading Color*, *Phys. Rev. Lett.* **126** (2021), no. 11 112001, [[arXiv:2007.09648](#)].
9. S. Höche, S. Mrenna, S. Payne, C. T. Preuss, and P. Skands, *A study of qcd radiation in vbf higgs production with vincia and pythia*, [arXiv:2106.10987](#).
10. T. Chen, T. M. Figy, and S. Plätzer, *NLO Multijet Merging for Higgs Production Beyond the VBF Approximation*, [arXiv:2109.03730](#).
11. B. Jäger, A. Karlberg, S. Plätzer, J. Scheller, and M. Zaro, *Parton-shower effects in Higgs production via Vector-Boson Fusion*, *Eur. Phys. J. C* **80** (2020), no. 8 756, [[arXiv:2003.12435](#)].
12. A. Buckley et al., *A comparative study of Higgs boson production from vector-boson fusion*, [arXiv:2105.11399](#).
13. J. R. Forshaw and M. Sjö Dahl, *Soft gluons in Higgs plus two jet production*, *JHEP* **09** (2007) 119, [[arXiv:0705.1504](#)].
14. R. Ángeles Martínez, M. De Angelis, J. R. Forshaw, S. Plätzer, and M. H. Seymour, *Soft gluon evolution and non-global logarithms*, *JHEP* **05** (2018) 044, [[arXiv:1802.08531](#)].
15. J. Bellm, G. Nail, S. Plätzer, P. Schichtel, and A. Siódmok, *Parton Shower Uncertainties with Herwig 7:*

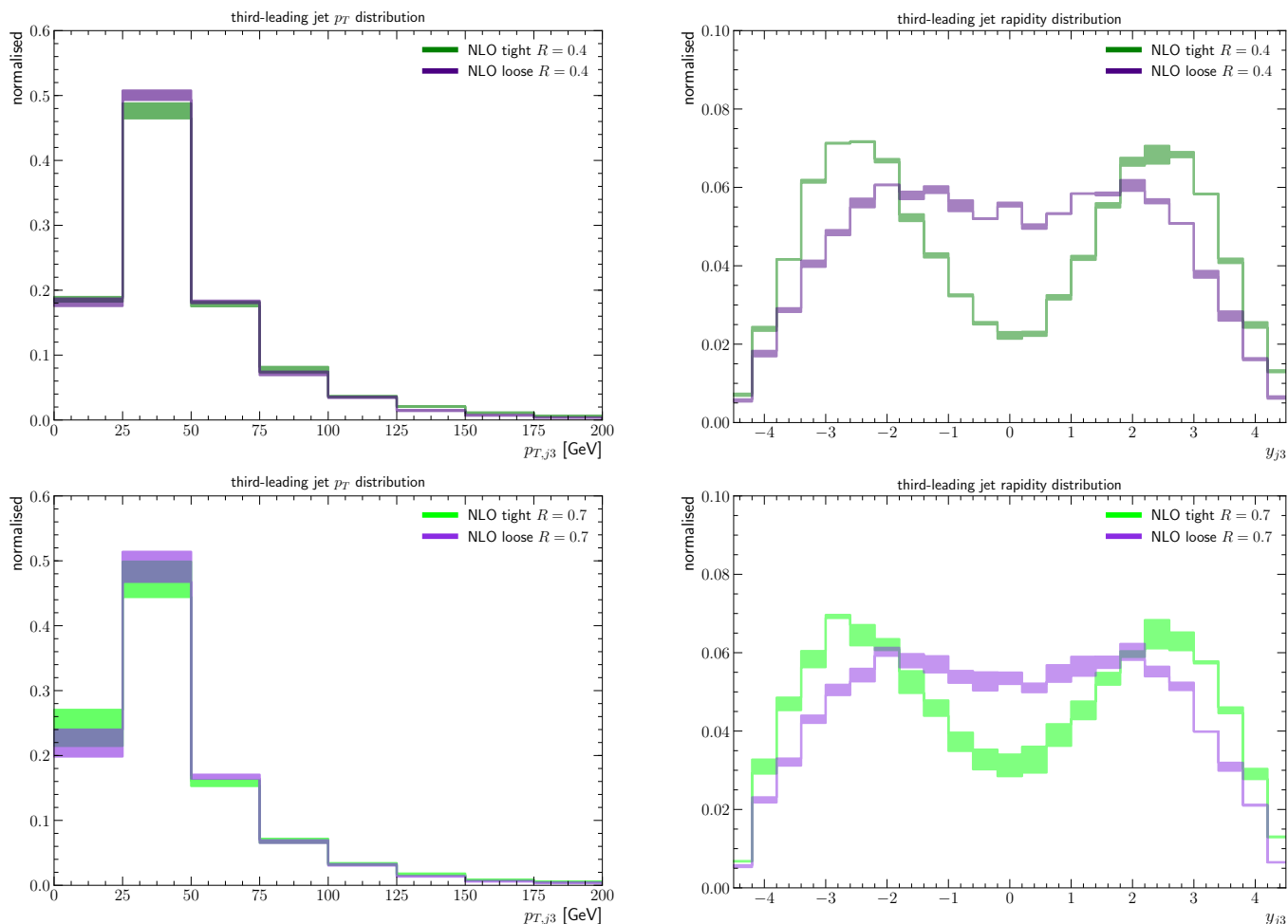


Fig. 4: A comparison of NLO VBS observables between the loose and tight selection cuts for a jet radius of  $R = 0.4$  (top plots) and  $R = 0.7$  (bottom plots). The transverse momentum (left plots) and rapidity (right plots) of the third-leading jet are shown. The bands constitute the outermost variations of the MPI model. The histograms have been normalised to the same area in each plot.

- Benchmarks at Leading Order, Eur. Phys. J. C* **76** (2016), no. 12 665, [arXiv:1605.01338].
16. J. Baglio et al., *Release Note - VBFNLO 2.7.0*, arXiv:1404.3940.
  17. J. Baglio et al., *VBFNLO: A Parton Level Monte Carlo for Processes with Electroweak Bosons – Manual for Version 2.7.0*, arXiv:1107.4038.
  18. K. Arnold et al., *VBFNLO: A Parton level Monte Carlo for processes with electroweak bosons*, *Comput. Phys. Commun.* **180** (2009) 1661–1670, [arXiv:0811.4559].
  19. M. Bähr et al., *Herwig++ Physics and Manual*, *Eur. Phys. J. C* **58** (2008) 639–707, [arXiv:0803.0883].
  20. J. Bellm et al., *Herwig 7.0/Herwig++ 3.0 release note*, *Eur. Phys. J. C* **76** (2016), no. 4 196, [arXiv:1512.01178].
  21. K. Cormier, S. Plätzer, C. Reuschle, P. Richardson, and S. Webster, *Parton showers and matching uncertainties in top quark pair production with Herwig 7*, *Eur. Phys. J. C* **79** (2019), no. 11 915, [arXiv:1810.06493].
  22. M. Rauch and S. Plätzer, *Parton-shower Effects in Vector-Boson-Fusion Processes*, *PoS DIS2016* (2016) 076, [arXiv:1607.00159].
  23. A. Buckley, H. Hoeth, H. Lacker, H. Schulz, and J. E. von Seggern, *Systematic event generator tuning for the LHC*, *Eur. Phys. J. C* **65** (2010) 331–357, [arXiv:0907.2973].
  24. M. Bähr, J. M. Butterworth, and M. H. Seymour, *The Underlying Event and the Total Cross Section from Tevatron to the LHC*, *JHEP* **01** (2009) 065, [arXiv:0806.2949].
  25. M. Bähr, S. Gieseke, and M. H. Seymour, *Simulation of multiple partonic interactions in Herwig++*, *JHEP* **07** (2008) 076, [arXiv:0803.3633].
  26. M. Bähr, J. M. Butterworth, S. Gieseke, and M. H. Seymour, *Soft interactions in Herwig++*, in *Proceedings, 1st International Workshop on Multiple Partonic Interactions at the LHC (MPI08): Perugia, Italy, October 27-31, 2008*, pp. 239–248, 2009. arXiv:0905.4671.
  27. S. Gieseke, F. Loshaj, and P. Kirchgaesser, *Soft and diffractive scattering with the cluster model in Herwig*, *Eur. Phys. J. C* **77** (2017), no. 3 156, [arXiv:1612.04701].
  28. J. Bellm, S. Gieseke, and P. Kirchgaesser, *Improving the description of multiple interactions in Herwig*, *Eur. Phys. J. C* **80** (2020), no. 5 469, [arXiv:1911.13149].

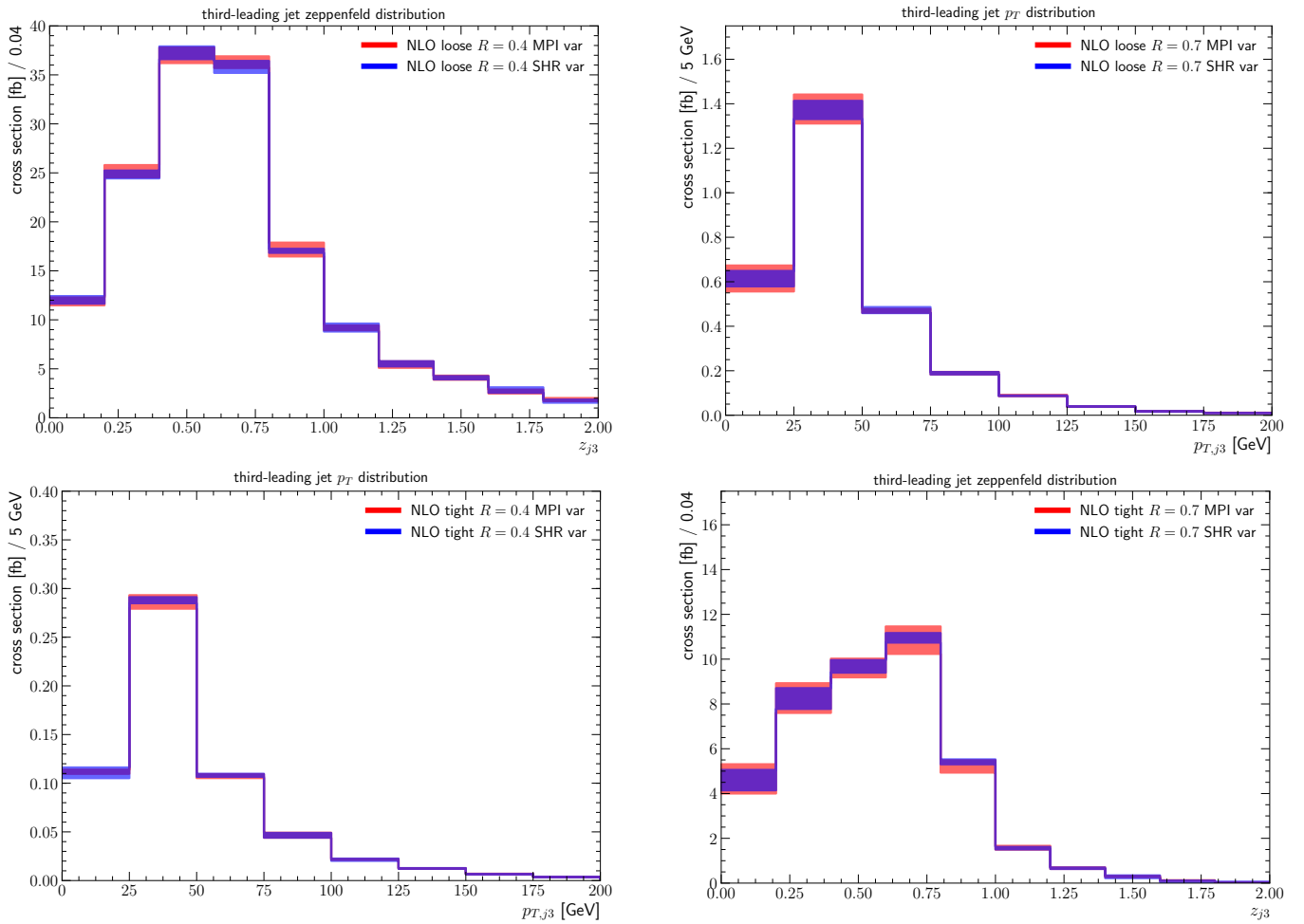


Fig. 5: A selection of comparisons of the MPI variations and shower variations for NLO VBS observables for the loose (top plots) and tight (bottom plots) selection cuts, for a jet radius of  $R = 0.4$  (left plots) and  $R = 0.7$  (right plots). The transverse momentum and Zeppenfeld variable of the third-leading jet are shown.

29. A. Donnachie and P. V. Landshoff, *Total cross-sections*, *Phys. Lett. B* **296** (1992) 227–232, [[hep-ph/9209205](#)].
30. S. Gieseke, C. Röhr, and A. Siódmok, *Colour reconnections in Herwig++*, *Eur. Phys. J. C* **72** (2012) 2225, [[arXiv:1206.0041](#)].
31. S. Gieseke, P. Kirchgaesser, and S. Plätzer, *Baryon production from cluster hadronisation*, *Eur. Phys. J. C* **78** (2018), no. 2 99, [[arXiv:1710.10906](#)].
32. A. Juste, S. Mantry, A. Mitov, A. Penin, P. Skands, E. Varnes, M. Vos, and S. Wimpenny, *Determination of the top quark mass circa 2013: methods, subtleties, perspectives*, *Eur. Phys. J. C* **74** (2014) 3119, [[arXiv:1310.0799](#)].
33. S. Argyropoulos and T. Sjöstrand, *Effects of color reconnection on  $t\bar{t}$  final states at the LHC*, *JHEP* **11** (2014) 043, [[arXiv:1407.6653](#)].
34. **ATLAS** Collaboration, M. Aaboud et al., *Charged-particle distributions in  $\sqrt{s} = 13$  TeV pp interactions measured with the ATLAS detector at the LHC*, *Phys. Lett. B* **758** (2016) 67–88, [[arXiv:1602.01633](#)].
35. S. Platzer and S. Gieseke, *Dipole Showers and Automated NLO Matching in Herwig++*, *Eur. Phys. J. C* **72** (2012) 2187, [[arXiv:1109.6256](#)].
36. J. Alwall, R. Frederix, S. Frixione, V. Hirschi, F. Maltoni, O. Mattelaer, H. S. Shao, T. Stelzer, P. Torrielli, and M. Zaro, *The automated computation of tree-level and next-to-leading order differential cross sections, and their matching to parton shower simulations*, *JHEP* **07** (2014) 079, [[arXiv:1405.0301](#)].
37. S. Plätzer, *Controlling inclusive cross sections in parton shower + matrix element merging*, *JHEP* **08** (2013) 114, [[arXiv:1211.5467](#)].
38. J. Bellm, S. Gieseke, and S. Plätzer, *Merging NLO Multi-jet Calculations with Improved Unitarization*, *Eur. Phys. J. C* **78** (2018), no. 3 244, [[arXiv:1705.06700](#)].
39. M. Cacciari, G. P. Salam, and G. Soyez, *The anti- $k_t$  jet clustering algorithm*, *JHEP* **04** (2008) 063, [[arXiv:0802.1189](#)].
40. **ATLAS** Collaboration, M. Aaboud et al., *Measurement of charged-particle distributions sensitive to the underlying event in  $\sqrt{s} = 13$  TeV proton-proton collisions with the ATLAS detector at the LHC*, *JHEP* **03** (2017) 157, [[arXiv:1701.05390](#)].
41. A. Buckley, J. Butterworth, D. Grellscheid, H. Hoeth, L. Lonnblad, J. Monk, H. Schulz, and F. Siegert, *Rivet*



*user manual*, *Comput. Phys. Commun.* **184** (2013)  
2803–2819, [[arXiv:1003.0694](https://arxiv.org/abs/1003.0694)].

42. Bittrich, Carsten and Kirchgaesser, Patrick and  
Papafstathiou, Andreas and Plätzer, Simon and Todt,  
Stefanie, “Soft QCD Effects in VBS/VBF Topologies.”  
<https://cern.ch/apapaefs/VBSQCD/>.